International Journal of Advanced and Multidisciplinary Engineering Science 2018, 2(1): 7-14
DOI: 10.5923/j.james.20180201.02

The Effect of Silver Nanoparticles on the Automotive-based Paint Drying Process: An Experimental Study

Hossein Lotfizadeh[1], Sajjad Rezazadeh[2], Mohammad Reza Fathollahi[3], Jalil Jokar[4], Abbasali Abouei Mehrizi[5], Babak Soltannia[1,*]

[1]Department of Mechanical Engineering, University of Alberta, Edmonton, Canada
[2]Department of Mechanical Engineering, Islamic Azad University, Takestan Branch, Takestan, Iran
[3]Department of Mechanical Engineering, KN Toosi University of Technology, Tehran, Iran
[4]Faculty of Art, Isfahan Art University, Isfahan, Iran
[5]Young Researchers and Elite Club, Karaj Branch, Islamic Azad University, Karaj, Iran

Abstract In this paper, the effects of nanoparticles on the paint-drying processes of automotive-based paints are investigated experimentally. For this purpose, rectangular aluminum plates covered by Alkyd Melamine (ES-665) car paint from Haviloox Company containing various amounts of 10 nm diameter silver nanoparticles from 0 to 25 ppm are prepared and tested in an airflow at velocities of 1.7 and 2.6 m/s parallel to the surface of the sample. The weights and temperatures of the painted plates are monitored during the experiments and the effects of the nanoparticles on paint-drying times are recorded. Using variations in air flow velocities, temperatures, and amounts of silver nanoparticles as important parameters in the drying process, an influence on the composition of the paint is indicated both during and at the end of the drying process, which would affect the quality of the final coating and improve the paint's chemical interactions. An average increase of 22% at the surface temperature of the samples and drying velocity is observed and recorded for the 10 ppm nano silver amount, indicating an optimal nanoparticle amount.

Keywords Silver nanoparticle, Paint, Drying, Automotive

1. Introduction

Automotive paint is a complex multi-component system designed to protect the frame of the vehicle and achieve the desired paint and finish. Each layer has a characteristic function and is comprised of a distinctive permutation of binders, resins, pigments, and additives [1]. The usage of nanotechnology as an emerging technology and particles in improving physical and chemical properties for better overall coating and more durable automotive clear coats has expanded in recent years as a consequence of considerable increases in market demand [2]. Since painting process is a complex and time-consuming process, several research projects have been carried out to investigate how to improve and facilitate the drying process due to the significant importance of this process in various industrial applications. Some of the main ones are mentioned below.

H. Lotfizadeh et al. [3] studied the effects of silver and copper nanoparticles on the wood-drying of poplar boards. It was concluded that nano metal particles have the potential to improve drying conditions and decrease drying stresses in convective kilns. Edmondstone et al. [4] utilized ATR-FTIR spectroscopy to characterize and investigate the visual features of a substantial collection of automotive clear coats. G. S. Hilton [5] concluded that an alkyd polymer paint viscosity, called "molecular weight", affected the paint generation in their understudy paint, with results revealing that a weaker paint was obtained due to lower viscous polymers. They also observed that their tinted paints required more drying time before the application had less paint. Romero and Alanı's study [6] used a detector for imaging and evaluating the statistics of dynamic speckle with a temporal average of the correlation function. In a similar study, Amalvya et al. [7] reported on the application of speckle interferometry for the drying of paints with relatively long drying times. Later, speckle interferometry was applied to systems with shorter drying times, such as spray paint systems. Yasui et al. [8] proposed a non-contact THz paint meter to monitor the dryness of a wet paint film

* Corresponding author:
soltannia@yahoo.com (Babak Soltannia)
Published online at http://journal.sapub.org/james

using a temporal profile of the THz pulse-echo signal. May and Porter [9] conducted a comparative evaluation of the analytical techniques used in the forensic examinations of paint, finding little correlation between the techniques.

Values of Young's modulus of free coating films were measured by G. Mirone et al. [10] to analyze the temporal development of the module of elasticity profile in water-borne alkyd coatings during the drying process of the coating films. They also developed a mathematical model to predict the degree of effective cross-linking and the mechanical behavior of the coating films with different thicknesses during the drying process.

Meanwhile, F. Buss et al. [11] investigated the effect of soluble polymer on the microstructure development in a drying particulate coating using a 1D model. They analyzed the effect of the polymer on the solution viscosity, diffusion, sedimentation, and evaporation. J. Domnick et al. [12] developed a simulation program which was able to analyze the heat-up process of a fully painted car body, including heat and mass transfer in water-based thin film coatings in the drying process of the automotive industry. G. Sheoran et al. [13] studied the drying process and detection of cracking/disbanding of the painted surface using a lens-less Fourier transform digital holographic interferometry and monitored the rate of the paint drying and the state of dryness and crack/disbond. In so doing, the researchers attempted to develop a model to predict the intermediate drying process of water-based paints on car bodies in continuous convective dryers.

During the same general time-frame, several experiments using industrial water-based paint systems and a model-based paint system applied on a sheet of metal were carried out by F. Brinckmann and P. Stephan [14] to validate the model. They monitored the sheet temperature and weight of the painted sheet at a rate of 1 Hz, and FTIR-spectroscopy was used to monitor the evaporation of the organic solvents during all experiments. Z. Wang et al. [15] experimentally demonstrated improvements in flame- and corrosion-resistance in a coating containing SiO_2 nanoparticles, including in salt spray conditions. It was concluded that in addition to improving corrosion resistance, a uniformly dispersed nano-SiO_2 particle nano-coating retains sufficient fire-resistant properties even after a 500 h salt spray test as a result of flame-retardant additives.

Furthermore, the effects of paint type, drying method and accelerated aging on paint stability in iris painting in ocular prostheses were investigated by M. Coelho Goiato et al. [16]. It was concluded that the oil paint, subjected to artificial aging under ultraviolet light, has the highest paint resistance in comparison with hydrosoluble acrylic, nitrocellulose automotive and hydrosoluble gouache, regardless of the drying method. S. H. Sonawane et al. [17] presented a novel methodology for synthesizing nano containers capable of responsive release of corrosion inhibitors using encapsulation. For all operating pH levels, the five wt% loading of nanocontainers proved to be practical and optimal for the sustained release of inhibitors for applications in marine coatings due to UV-spectroscopy at different pH levels, corrosion rate analysis, and TAFEL plots of nanocontainer coatings.

P. A. Stuiver and G. T. Barkema [18] studied the distribution pattern of pigments in a solvent-based paint after the introduction of water-based pigment dispersion. Their model was able to evaluate several influential thermodynamic and kinetic factors through biased diffusion of the three types of lattice particles with species-dependent mobility, using Monte Carlo simulations. The results elucidated the decisive role of kinetic processes in reaching homogeneous distribution, regardless of unfavorable equilibrium conditions. C. H. Hodges et al. [19] studied the effects of nanoparticle shape on spherical Ludox silica and disk-like laponite clay deposit structures. The application of dark-field optical microscopy and atomic force microscopy revealed the crucial importance of both shape and concentration of nanoparticles in determining the structural properties of the final dried nanoparticle deposit.

N. Tahmassebi et al. [20] used a series of analytical techniques to evaluate the effects of nano silica on the viscoelastic properties and scratch morphologies of certain clear coats. The authors found that increasing the amount of hydrophobic nano silica particles introduced into an automotive clearcoat results in a progressive transition from fracture-type scratches to plastic-type scratches, together with an increased toughness, while decreasing the glass transition temperature (T_g). B. Ramezanzadeh et al. [21] conducted an experimental analysis of the scratch-resistance and mechanical properties of an acrylic/melamine clearcoat on black and silver basecoats. The accelerated weathering and xenon exposure tests showed higher scratch resistance in the silver sample compared to the black one, whereas the scratch-resistance of both the black and silver samples was improved at short exposure times.

In other work, M. Baneshi et al. [22] proposed an optimized design method of pigmented coatings which controls the material, size and concentration of pigment particles to obtain the desired thermal and aesthetical characteristics. Maximizing the reflectance of the near-infrared (NIR) region in the thermal effects while keeping the dark tone through a minimized visible (VIS) reflection greatly improved the efficiency of the suggested optimum coatings. In this regard, optimum cupric oxide particles proved to have a better performance than TiO_2 and Cu_2O. R. Consiglio et al. [23] improved the mechanical properties of polymer coatings, especially their scratch- and mar-resistance, which can be applied to produce ultrathin hard coatings for protective overcoats in the magnetic storage industry. The results confirmed the application of their method for accurate characterization of elasticity, hardness, adhesion and mechanical integrity with high reproducibility. H. Yari et al. [24] applied artificial weathering exposure tests on silver and black basecoats to analyze the effect of basecoat pigmentation on mechanical features of an automotive basecoat/clearcoat system.

The effect of nano-silica particles on the protective

performance of polyurethane coatings was investigated by D. J. Mills et al. [25]. This study focused on the effect of non-polar nano-silica particles on electrochemical characteristics of 2-pack polyurethane matrix. The Taber abrasion test showed that abrasion resistance could be improved either by introducing nano-silica particles or by higher curing temperatures. S. Pouladi et al. [26] introduced a novel electroplating bath. The number of coating cracks was used to identify the optimum bath composition. The analysis of mechanical properties of nanocomposite coatings in operating conditions confirmed that the nanocomposite coatings have a lower weight loss compared to the Ni–Zn–P coatings.

B. Ahmadi et al. [27] investigated the effect of nano layered silicates on the properties of an automotive refinish clear coat based on polyurethane. The optimum nano-filler/polymer ratio was obtained using standard methods like adhesion, impact and bending tests together with scratch and mar resistance tests. The results indicated a 10% increase in gloss retention in the presence of only three wt% of nano-filler. Z. Ranjbar and S. Rastegar [28] studied different responses of the coatings to the marring stress and critical forces using the nano-indenter technique. In this study, the presence of nano-silica in the coating formulation led to decreases in the plastic deformation compared to the elastic part and the damage width.

Z. Ranjbar et al. [29] studied the curing reaction of a thermosetting acrylic-melamine clear-coat in the presence of nano-silica particles with different surface modifications. The results elucidated that, besides the extensive effects on the film morphology, the activation energy of cure reduces as a result of introducing either hydrophilic or hydrophobic nano-silica particles, while the total heat of reaction increases. E. Scrinzi et al. [30] studied the influence of nano-silica particles on properties of clear coats using three different double component isocyanate/polyol clear coats exposed to artificial weathering. Detailed analysis of scratch and mar resistance, morphology and aesthetic properties proved the application of nano-fillers as an efficient technique to increase the abrasion resistance without affecting the optical clarity of high gloss coatings.

In this paper, the effect of silver nanoparticles on the drying process of Alkyd Melamine (ES-665) car paint was experimentally tested and the parameters affecting the samples drying rate were analyzed.

2. Experiment

2.1. Material and Sample Preparation

Experimental results were carried out using spherical and monodispersed silver nanoparticles with a nominal diameter of 10 nm due to their superior thermal conductivity. The base paint employed for the test was Alkyd Melamine (ES-665) car paint, manufactured by Haviloox Company. An aqueous nanosilver (NS) suspension was produced through the application of an electrochemical technique in cooperation with Iran Nanopooshesh Company. In the nanoparticle manufacturing, de-ionized water was used as a starter, NaBH4 as a reducing agent, and TADDD as a stabilizer.

The paints were prepared at six different nanoparticle amounts. As the effects of the nanoparticle on the drying process was determined without the use of nanoparticles, they were neglected in the first paint, in other words the results have been normalized with respect to the baseline paint category which contains no silver nanoparticles. Hence, for validation, only normalized results of nano-enhanced paints are compared to each other. The other paint was made with 0.005, 0.0010, 0.0015, 0.0020 and 0.0025 ppm of silver nanoparticles (nanoparticle concentration being reported in ppm) to study the effect of viscosity and at the same time figure out the optimum amount of nanoparticle resulting in the fastest drying process. To obtain a nano-solution with the exact percentage of the base paint and nanoparticles, the weight of the samples was measured directly after the paint application and the drying process using a digital balance. To decrease the potential error, tests were repeated twice.

The nano-solution was prepared using nanoparticles of silver, Alkyd Melamine as the base paint, and Toluene as the solvent. An optical image of the silver nanoparticles at the base paint is shown in Fig. 1.

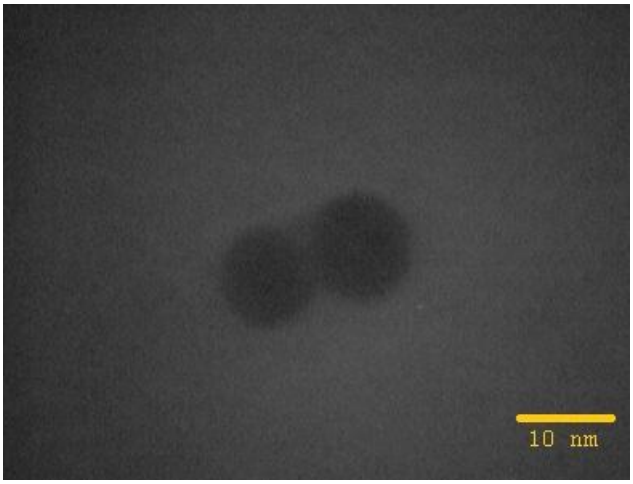

Figure 1. Silver nanoparticles at the base paint

Rectangular flat aluminum plates were coated with nano-made paint solutions and dried in an oven, which is considered a relevant paint-drying process. For this purpose, the sample surfaces were first degreased using acetone liquid. The surfaces were then immersed in NaOH for 50 seconds and washed with water, followed by immersion in nitric acid for 5 seconds. Finally, the surfaces were etched with H_2SO_4 acid to ensure proper coating and absence of debris. The plates were tested in laminar flow with two different air velocities of 1.7 and 2.6 m/s parallel to the surface of samples to study the effect of air velocity on drying rate, if there is any.

The tests were performed in a subsonic wind tunnel with a surface section of 475mm × 495 mm, a three-phase radial

flow jet fan with a power of 3 KW, and a filter to remove the dust particles. The error of air uniformity was 5%. The flow velocity was also measured by an ST-618 B thermomanometer, which ensured the accuracy of the flow velocity during the tests. The air flow humidity was controlled and measured by two SDG psychrometers located at the air inlet and outlet, and the temperature was measured using PT-100 thermocouple sensors located in the testing section, with an accuracy of ±0.1℃. A laser thermocouple was also used to measure the surface temperatures of the samples. A photo of the wind tunnel utilized during the tests is shown in Fig. 2.

Figure 2. Wind tunnel used for tests

2.2. Testing

The wind tunnel section was first heated by digital heaters. To enable accurate comparison of results, a constant reference temperature (24.5℃) was applied. After reaching the constant temperature and air flow velocity, the samples were inserted into the testing section and tested.

3. Results and Discussion

During the tests, the temperature, air velocity and weight of the samples were all recorded. The temperature of the sample surfaces with different amounts of nanoparticles is shown in Table 1.

Considering the reports in Table 1, the results of the tested samples with the same amounts of nanoparticles at different air flow velocities indicate the effect of the convection velocity on the temperature of the samples surfaces. The temperatures of the samples are equal at the beginning of the tests (t=0), but when the drying process begins, the temperature of the coated and non-coated samples increases, which is higher at an air velocity of 1.7m/s. This means that the air velocity is an effective parameter in the drying velocity of the samples; in other words the increase of the Reynolds number (Re) decreases the drying process rate, which was predictable.

The maximum surface temperature was observed at 80.5℃ in the nanoparticle amount of 10 ppm at the air velocity of 1.7 m/s, which illustrates the highest drying process rate. Compared to a maximum surface temperature of 69℃ at an air velocity of 2.6 m/s and a nanoparticle amount of 10 ppm, an increase of 16.66% in the temperature of the samples surfaces was obvious. Comparing samples with the same amount of nanoparticles at two different air velocities indicates an average increase of 21.6% in the maximum surface temperatures.

The solvent vaporization indicates a mass transformation in the surface area and air flow of the boundary samples. Furthermore, in considering the Wv as the vaporized paint solvent weight and Ws as the dried paint weight which the paint mass on the samples finally reaches, the paint film weight variations (the Wv/Ws ratio) that occurred in the course of the drying process were also measured with a digital balance. The reported measurements are shown in Table 2.

The effect of air flow velocity on the paint film weight variations is obvious in Table 2. In noting the Wv/Ws ratio of the coated samples in specific amounts of nanoparticles with different air velocities, it is clear that the increase in the Reynolds number (Re) decreases the drying velocity of the samples, indicating a delay in the drying process.

Table 1. Surface Temperature of Samples (℃)

Time (min)		0	4	8	12	16	20	24	28	32	36	40	44
Temperature at 0 ppm	v=1.7 m/s	24.5	33	35	38	59	70	75	77	78	78.5	79	79.5
	v=2.6 m/s	24.5	30	31	32	35	48	57	61	64	64	64.5	65
Temperature at 5 ppm	v=1.7 m/s	24.5	35	39	44	62	73	77.5	78.5	79	80	80.5	80
	v=2.6 m/s	24.5	30	33	35	41	52	62	65	65.5	66	66.5	67
Temperature at 10 ppm	v=1.7 m/s	24.5	37	41	56	73	80	79.5	80	80.5	80	80	80.5
	v=2.6 m/s	24.5	32	35	37	53	63.5	67	67.5	68	68.5	68.5	69
Temperature at 15 ppm	v=1.7 m/s	24.5	36	39	45	65	74	76	78	79.5	80	79.5	80
	v=2.6 m/s	24.5	29	32	33	37	50	62	65	65.5	66	66	66.5
Temperature at 20 ppm	v=1.7 m/s	24.5	34	36	39	41.5	54	68	74	77	78	77.5	78
	v=2.6 m/s	24.5	28	30	31	33	35	47	53	60	62.5	63	63.5
Temperature at 25 ppm	v=1.7 m/s	24.5	33	35	37	39.5	55	64	71	75.5	76	77	77.5
	v=2.6 m/s	24.5	27	28	30	32	34	46	54	58	59	60	60.5

Table 2. Variations in Wv/Ws Ratio of Samples

Time(min)		0	4	8	12	16	20	24	28	32	36	40	44
Wv/Ws at 0 ppm	v=1.7 m/s	0.185	0.108	0.081	0.057	0.050	0.034	0.019	0.011	0.007	0.0	0.0	0.0
	v=2.6 m/s	0.215	0.133	0.118	0.082	0.057	0.066	0.051	0.021	0.006	0.003	0.0	0.0
Wv/Ws at 0.0005 ppm	v=1.7 m/s	0.263	0.083	0.055	0.041	0.045	0.037	0.017	0.003	0.0	0.0	0.0	0.0
	v=2.6 m/s	0.238	0.045	0.024	0.015	0.011	0.005	0.003	0.001	0.0	0.001	0.0	0.0
Wv/Ws at 0.0010 ppm	v=1.7 m/s	0.353	0.093	0.058	0.039	0.006	0.0	0.0	0.002	0.0	0.0	0.002	0.0
	v=2.6 m/s	0.362	0.043	0.010	0.006	0.003	0.001	0.0	0.006	0.013	0.013	0.025	0.0
Wv/Ws at 0.0015 ppm	v=1.7 m/s	0.406	0.131	0.101	0.074	0.048	0.026	0.0	0.0	0.0	0.002	0.004	0.0
	v=2.6 m/s	0.279	0.062	0.048	0.028	0.014	0.011	0.004	0.0	0.0	0.003	0.001	0.0
Wv/Ws at 0.0020 ppm	v=1.7 m/s	0.543	0.094	0.068	0.044	0.032	0.020	0.004	0.0	0.004	0.002	0.0	0.002
	v=2.6 m/s	0.661	0.198	0.139	0.119	0.097	0.068	0.034	0.060	0.0	0.0	0.004	0.0
Wv/Ws at 0.0025 ppm	v=1.7 m/s	0.480	0.109	0.089	0.078	0.068	0.047	0.035	0.020	0.0	0.002	0.004	0.0
	v=2.6 m/s	0.428	0.087	0.060	0.036	0.032	0.030	0.013	0.013	0.001	0.0	0.013	0.001

Since the paint film containing the paint, solvent, and nanoparticles attaches the air as the gas phase in a permanent convection situation in the wind tunnel, a stable film begins to be formed. The solvent vaporization from the surface of the paint film against the air convection during the drying process causes an increase in the temperature of the samples and the surrounding air. The temperature increase of the paint systems at an air velocity of 1.7 m/s for different amounts of nanoparticles is shown in Fig. 3, while Fig. 4 shows the paint film sample temperatures increase versus time for an air velocity of 2.6 m/s.

It is obvious that higher temperatures of the sample surfaces make the drying process proceed at a higher rate. Silver nanoparticles decrease the needed energy and improve the time needed for the drying process, since silver is a metal with a higher thermal conductivity than the base paint. When the amount of nanoparticles increases, the total conductivity of the nano-coated surfaces improves, which causes an increase in temperature of the sample surfaces and thus a higher drying process. This improvement in conductivity occurs in nanoparticle amounts ranging from 0 ppm to 10 ppm. Figures 3 and 4 show that the coated samples with 10 ppm silver nanoparticles have the highest surface temperatures at air velocities of 1.7 and 2.6 m/s, which means that paint with a 10 ppm nanoparticle amount has the best conductivity coefficient and thus the highest paint-drying velocity occurs. However, a nanoparticle amount of more than 10 ppm in the base paint decreases the temperature of the samples, which can be attributed to viscosity augmentation (entropy mitigation). Another possible reason could be the increase in nanoparticle content results in more agglomeration and consequently decreasing the effective conductivity of nanoparticles.

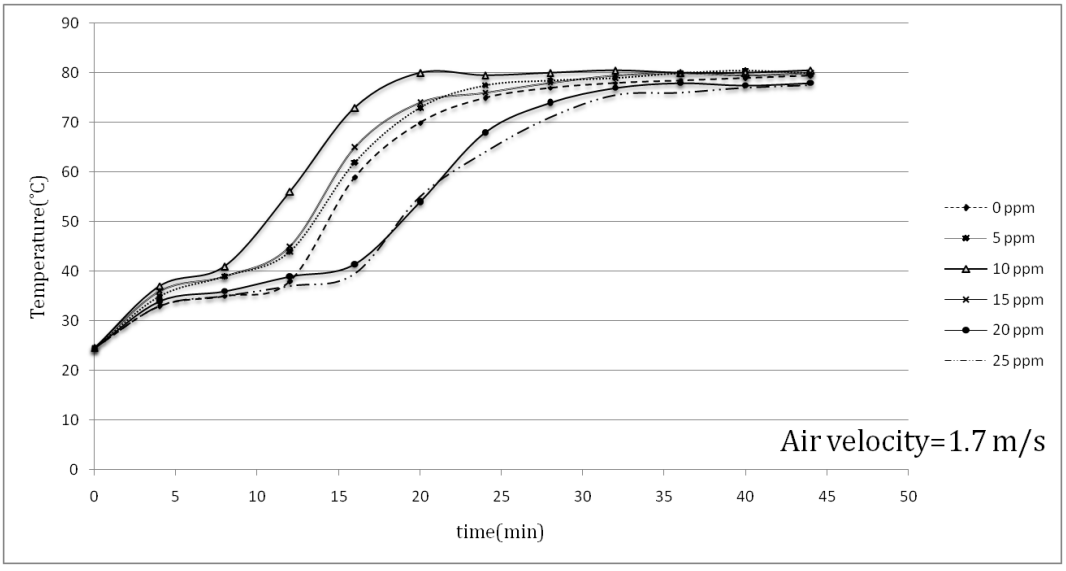

Figure 3. Temperature increase in painted samples during a drying process at v=1.7 m/s

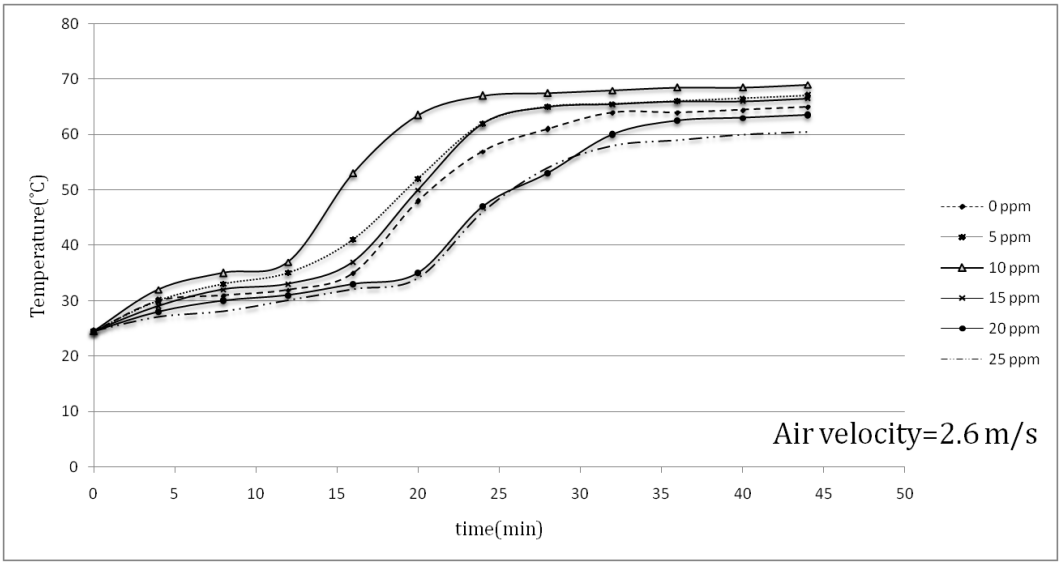

Figure 4. Temperature increase in painted samples during a drying process at v=2.6 m/s

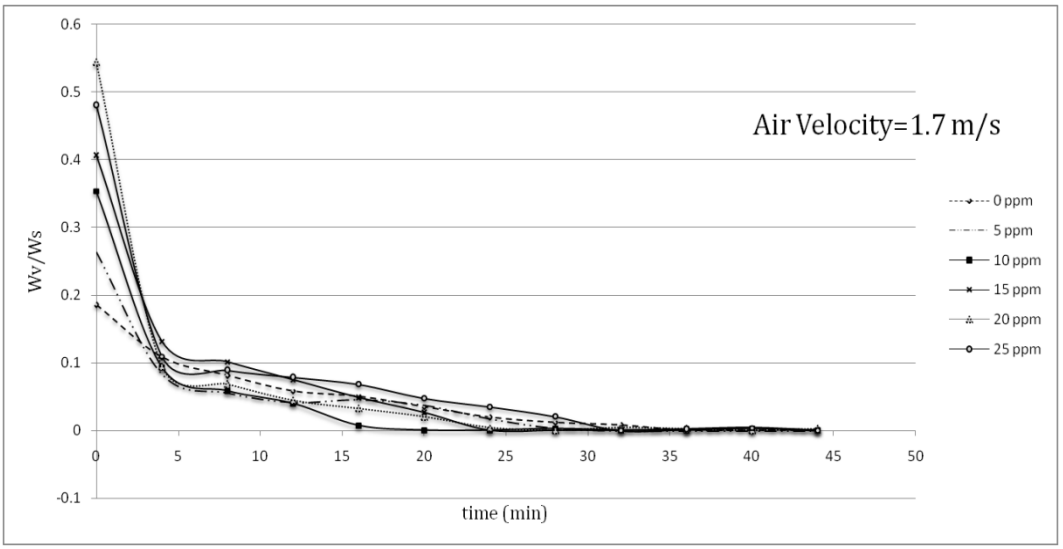

Figure 5. Decrease in sample paint weight in drying process at v=1.7 m/s

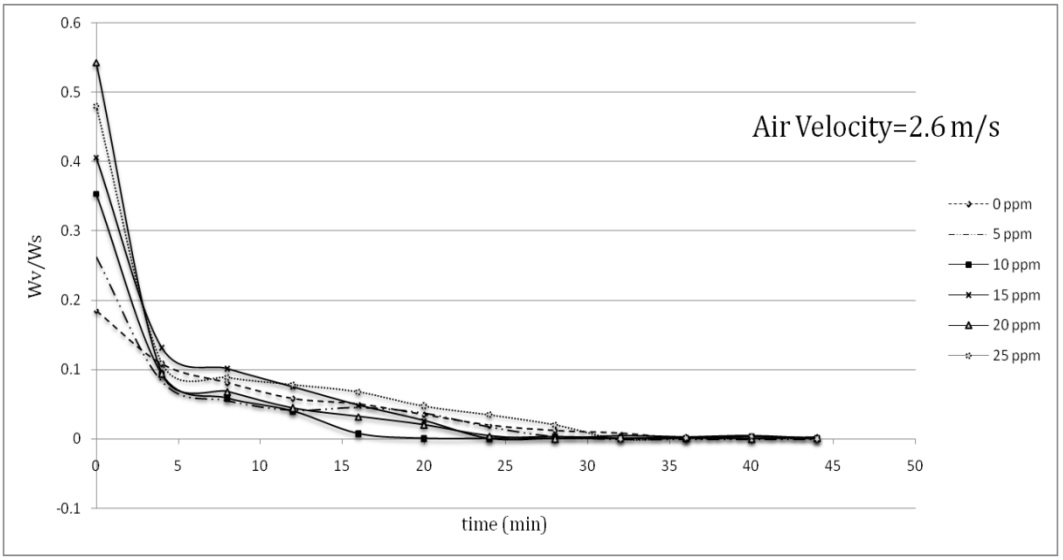

Figure 6. Decrease in sample paint weight in drying process at v=2.6 m/s

Because the paint film weight variations (Wv/Ws) decrease the drying process, and since Ws is a fixed amount, the decrease shows the vaporization of the solvent in the samples. This ratio is applied as a non-dimensional parameter that is useful for all studies. For better comparison, the paint films with different amounts of silver nanoparticles at the same air flow velocities are presented separately in Figs. 5 and 6. Figure 5 shows the sample paint film weight decrease versus time at an air velocity of 1.7 m/s, along with different amounts of nanoparticles. Figure 6 shows the sample paint film weight variation during the drying process at an air velocity of 2.6 m/s.

The greatest reduction in Wv/Ws can be seen at 10 ppm in Figs. 5 and 6, which was expected.

The curves from Fig. 3 to Fig. 6 show two stages in the drying process of the samples. In the first stage, the ascent of the surface temperatures and the descent of Wv/Ws in the samples are transient, while in the second stage, the surface temperatures of the samples and Wv/Ws reach a stable level. In the first stage, the sample temperature and Wv/Ws ratio are transient when the solvent vaporization continuously takes place (the rate for which is noticeable at the beginning of the tests and then starts to fluctuate with the passing of time). When the solvent vaporization is completed, the paint film reaches its solid form, and the sample temperatures and Wv/Ws rates become stable, as can be seen in the figures for the second stage.

It should be noted that the coated samples seem to be heavier at higher air velocities compared to lower air velocities, which could be due to the drag force of the plates causing an extra load; therefore, more weight on the digital balance can be estimated as an error.

4. Conclusions

Aluminum plates coated with Alkyd Melamine (ES-665) car paint containing silver nanoparticles with a diameter of 10 nm were tested in a wind tunnel using two different air velocities parallel to the aluminum plate surfaces. During the experiments, which took place at a constant heat flux of the wind tunnel test section and laminar air flow, the temperature of the sample surfaces was monitored and the mass-loss ratio due to the evaporation of the solvents at the boundary area of the sample surfaces with the flowing air was noted.

Applying two different air convection velocities of 1.7 and 2.6 m/s, it was consequently found that the Reynolds number had an inverse effect on the temperatures of the coated samples surfaces and the solvent vaporization velocities in the drying process, showing that a 52.94% increase in the Reynolds number decreased the maximum temperatures of the samples 21.6% on average.

The effect of the silver nanoparticle amount on the drying process of the samples was also investigated by using paint with five different amounts of nanoparticles (5, 10, 15, 20, 25 ppm) and paint without nanoparticles. In the tests, the paint with 10 ppm silver nanoparticles showed the best performance results for the drying process, in which the maximum temperature of 80.5℃ at an air velocity of 1.7 m/s and a maximum temperature of 69℃ at an air velocity of 2.6 m/s was reported. The best solvent vaporization was also observed at this nanoparticle amount, which is likely due to the higher thermal conductivity of silver than the base paint leading to an improvement of the paint's total thermal conductivity. Additionally, although the silver nanoparticles increased a specific surface area of the heat transformation, increases of more than 10 ppm nanoparticles had an inverse effect on both sample surface temperature and solvent vaporization rate. It appears that increase in viscosity (reduction in entropy) is responsible for the conflict here due to the restricted movement of the molecules.

The present study reported a useful approach to improving the automotive-based paint-drying process as well as other properties of coated aluminum plates. It also reveals the importance of nano usage for improving a material's characteristics. The higher the convection coefficient and the lower diameter of the nano particles, the better the results of the paint-drying process. The effects of air convection turbulence can also be derived from these results. This enhancement in paint-drying rate justifies the inclusion of nanoparticles, requiring less time and consequently having economic justifications.

REFERENCES

[1] Bentley, J. Composition, manufacture and use of paint. In *Forensic Examination of Glass and Paint Analysis and Interpretation.* B. Caddy (Ed.), Taylor & Francis: London; 2001, 123-141.

[2] Jalili, M. M. Moradian, S. Deterministic performance parameters for an automotive polyurethane clear coat loaded with hydrophilic or hydrophobic nano-silica. *Progress in Organic Coatings*; 2009, 66, 359-366.

[3] Lotfizadeh, H. Shahverdi, M. Dashti, H. Taghiyari, H. R. Potential Usage of Nanotechnology in Wood Drying: Treating Poplar Boards with Nano metals Affects the Drying Behavior, *Digest Journal of Nano materials and Bio structures.* Vol. 7, No. 4; 2012, 1627-1637.

[4] Edmondstone, G. Hellman, J. Legate, K. Vardy, G.L. Lindsay, E. An assessment of the evidential value of automotive paint comparisons, *J. Can. Soc. Forensic Sci;* 2004, 37, 147-153.

[5] Hilton, G.S. Proceedings of the 17th FATIPEC Congress, 1984, 317.

[6] Romero, G.G. Alanıs, E.E. Statistics of the dynamic speckle produced by a rotating diffuser and its application to the assessment of paint drying. *J. Opt Eng;* 2000, 39, 1652-1658.

[7] Amalvya, J. I. Lasquibar, C. A. Arizaga, R. Rabal, H. Trivi, M. Application of dynamic speckle interferometry to the drying of coatings. *J. Prog Org Coat;* 2001, 42, 89-99.

[8] Yasui, T. Yasuda, T. Sawanaka, K.I. Araki, T. Tetrahertz paint meter for non-contact monitoring of thickness and

drying progress in the paint film. *J. Appl Opt;* 2005, 44, 6849-6856.

[9] May, R. W. Porter, J. An Evaluation of Common Methods of Paint Analysis. *J. Forens. Sci. Soc;* 1975, 15, 137.

[10] Mirone, G. Marton, B. Julius, G. Vancso, G. Elastic modulus profiles in the cross sections of drying alkyd coating films: modeling and experiments. *J. European Polymer;* 2004, 40, 549-560.

[11] Christine, F. B. Roberts, C. Kathleen, C. Crawford, S. Peters, K. Lorraine, Francis, F. Effect of soluble polymer binder on particle distribution in a drying particulate coating. *J. Colloid and Interface Science.*; 2011, 359, 112-120.

[12] Domnick, J. Gruseck, D. Pulli, K. Scheibe, A. Ye, Q. Brinckmann, F. Investigations of the drying process of a water-based paint film for automotive applications. *Chemical Engineering and Processing;* 2011, 50, 495-502.

[13] Sheoran, G. Sharma, S. Shakher. C. Monitoring of drying process and cracking/disbonding of paints using lensless Fourier transform digital holography. *J. Optics and Lasers in Engineering;* 2011, 49, 159-166.

[14] Brinckmann, F. Stephan, P. Experimental investigation of the drying process of water-based paints used in automotive industry. *J. Chemical Engineering and Processing;* 2011, 50, 489-494.

[15] Wang, Z. Han, E. Liu F. Ke, W. Fire and Corrosion Resistances of Intumescent Nano-coating Containing Nano-SiO_2 in Salt Spray Condition. *J. Mater. Sci. Technol*; 2010, 26(1), 75-81.

[16] Goiato, M. C. Fernandes, A. U. R. Dos Santos, D. M. Haddad, M. F. Moreno, A. Pesqueira, A. A. Alteration of blue pigment in artificial iris in ocular prosthesis: Effect of paint, drying method and artificial aging. *J. Contact Lens and Anterior Eye*; 2011, 34, 22-25.

[17] Sonawane, S. H. Bhanvase, B. A. Jamali, A. A. Dubey, S. K. Kale, S. S. Pinjari, D. V. Kulkarni, R. D. Gogate, P. R. Pandit. A. B. Improved active anticorrosion coatings using layer-by-layer assembled ZnO nano-containers with benzotriazole. *J. Chemical Engineering*; 2012, 189-190, 464-472.

[18] Stuiver, A. Barkema, G.T. Simulations of color development in tinted paints. *J. Colloid and Interface Science;* 2010, 344, 256–260.

[19] Hodges, C. S. Ding, Y. Biggs, S. The influence of nano particle shape on the drying of colloidal suspensions. *J. Colloid and Interface Science.*; 2010, 352, 99-106.

[20] Tahmassebi, N. Moradian, S. Ramezanzadeh, B. Khosravi, A. Behdad, S. Effect of addition of hydrophobic nano silica on viscoelastic properties and scratch resistance of an acrylic/melamine automotive clear coat. *J. Tribology International;* 2010, 43, 685–693.

[21] Ramezanzadeh, B. Moradian, S. Yari, H. Kashani, A. Niknahad, M. The effect of base coat pigmentation on the scratch resistance and weathering performance of an acrylic–melamine base coat/clear coat automotive finish. *J. Tribology International;* 2012, 47, 77-89.

[22] Baneshi, M. Maruyama, S. Komiya, A. Comparison between aesthetic and thermal performances of copper oxide and titanium dioxide nano-particulate coatings. *J. Quantitative Spectroscopy & Radiative Transfer;* 2011, 112, 1197-1204.

[23] Consiglio, R. Randall, N.X. Bellaton, B. Von Stebut, J. The nano-scratch tester (NST) as a new tool for assessing the strength of ultrathin hard coatings and the mar resistance of polymer films. *Thin Solid Films;* 1998, 332, 151-156.

[24] Yari, H. Moradian, S. Ramazanzade, B. Kashani, A. Tahmasebi, N. The effect of basecoat pigmentation on mechanical properties of an automotive basecoat/clearcoat system during weathering. *Polymer Degradation and Stability;* 2009, 94, 1281-1289.

[25] Mills, D. J. Jamali, S. S. Paprocka, K. Investigation into the effect of nano-silica on the protective properties of polyurethane coatings. *Polymer Degradation and Stability;* 2009, 94, 1281-1289.

[26] Pouladi, S. Shariat, M. H. Bahrololoom, M. E. Electrodeposition and characterization of Ni–Zn–P and Ni–Zn–P/nano-SiC coatings. *Surface & Coating Technology;* 2012, 213, 33-40.

[27] Ahmadi, B. Kassiriha, M. Khodabakhshi, K. Mafi, E. R. Effect of nano layered silicates on automotive polyurethane refinish clear coat. *Progress in Organic Coatings;* 2007, 60, 99-104.

[28] Ranjbar, Z. Rastegar, S. Evaluation of mar/scratch resistance of a two-component automotive clear coat via nano-indenter. *Progress in Organic Coatings*; 2009, 64, 387-391.

[29] Ranjbar, Z. Jannesari, A. Rastegar, S. Montazeri, S. Study of the influence of nano-silica particles on the curing reactions of acrylic-melamine clear-coats. *Progress in Organic Coatings;* 2009, 66, 372-376.

[30] Scrinzi, E. Rossi, S. Kamarchik, P. Deflorian, F. Evaluation of durability of nano-silica containing clear coats for automotive Applications. *Progress in Organic Coatings;* 2011, 71, 384-390.